Eur. Phys. J. A **26**, 209–220 (2005)
DOI 10.1140/epja/i2005-10162-7

THE EUROPEAN PHYSICAL JOURNAL A

On the treatment of the Δ-contributions in electromagnetic pp-knockout reactions

C. Giusti[1], F.D. Pacati[1], M. Schwamb[2,a], and S. Boffi[1]

[1] Dipartimento di Fisica Nucleare e Teorica, Università degli Studi di Pavia, and Istituto Nazionale di Fisica Nucleare, Sezione di Pavia, I-27100 Pavia, Italy
[2] Institut für Kernphysik, Johannes Gutenberg-Universität Mainz, D-55099 Mainz, Germany

Received: 29 July 2005 /
Published online: 16 November 2005 –
Communicated by G. Orlandini

Abstract. The treatment of the Δ-current and its contribution in the exclusive $^{16}\mathrm{O}(e,e'pp)^{14}\mathrm{C}$ and $^{16}\mathrm{O}(\gamma,pp)^{14}\mathrm{C}$ knockout reactions are investigated in combination with the effects of correlations. Different parametrizations of the effective Δ-current and different treatments of correlations in the two-nucleon overlap function are considered. The results are presented and discussed for a suitable choice of kinematics. It is found that the investigation of different mutually supplementing kinematics is necessary to resolve the uncertainties in the theoretical ingredients and extract clear and unambiguous information on correlations.

PACS. 21.60.-n Nuclear structure models and methods – 25.20.Lj Photoproduction reactions – 25.30.Fj Inelastic electron scattering to continuum

1 Introduction

The independent particle shell model, describing a nucleus as a system of nucleons moving in a mean field, can reproduce many basic features of nuclear structure. It is, however, nowadays understood that the repulsive core of the NN-interaction induces additional short-range correlations (SRC) which are beyond a mean-field description. SRC have a decisive influence on the spectral distribution of nucleons and on the binding properties of atomic nuclei. A powerful tool for the study of SRC are electromagnetically induced two-nucleon knockout reactions like (γ, NN) or $(e, e'NN)$ because the probability that a real or a virtual photon is absorbed by a nucleon pair should be a direct measure for SRC (for an overview, see [1]). However, this simple picture is modified by the competing mechanisms which may additionally contribute to two-nucleon knockout due to their two-body character. At low and intermediate energies, the most important ones are those due to two-body meson-exchange (MEC) and Δ currents, as well as to final-state interactions (FSI). The latter consist in principle of two different contributions, namely the mutual interaction of the two emitted nucleons (NN-FSI), which can be described by a realistic NN-interaction [2,3], and the interaction of each of the two outgoing nucleons with the residual nucleus, which is described in our model by a suitable optical potential. Whereas NN-FSI depend strongly on the kinematics and on the chosen electromagnetic probe [2,3], the N-nucleus interaction generally represents the main contribution of FSI and can never be neglected. The optical potential always leads to a strong reduction of the calculated cross-section leaving, however, its main qualitative features unchanged [2–4]. Moreover, the model dependence due to the specific choice of a realistic optical potential turns out to be small [1,4].

Concerning the two-body currents, the nonrelativistic pion-in-flight and seagull MEC contributions (see fig. 1) are forbidden in pp-knockout. Therefore, the only electromagnetic background mechanism we have to deal with in pp-knockout is the Δ-current, consisting of an excitation and a de-excitation part (fig. 1).

It was found in previous studies [1,5–12] that the relevance of the Δ-contribution depends strongly on the kinematics and on the particular final state of the residual nucleus, as well as on the type of electromagnetic probe. It is possible to envisage specific situations where either the contribution of the one-body or of the two-body Δ-current is dominant. A combined study of both types of situations may provide an interesting tool to disentangle and separately investigate the two reaction processes.

If one is primarily interested in studying correlations, situations and kinematics should be preferred where the Δ-contribution is as small as possible, because the remaining one-body contribution can only contribute via correlations in the initial or in the final state, and should

[a] e-mail: schwamb@kph.uni-mainz.de

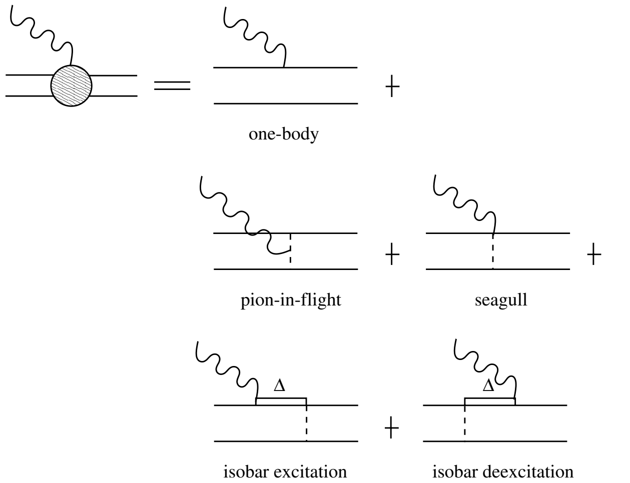

Fig. 1. The electromagnetic currents contributing to two-nucleon knockout reactions at low and intermediate energies.

therefore be maximized in order to have the most direct access to SRC.

In any case, a conceptual satisfying description of the behavior of the Δ in the nuclear medium is necessary. This would also require a consistent treatment of nucleonic as well as of Δ degrees of freedom in the two-body overlap function in the initial as well as in the final state which is, however, not available at present. Therefore, one has to rely on approximative schemes.

The central aim of the present paper is a systematic study of different tractable parametrizations of the Δ-current and of their contribution to pp-knockout off complex nuclei in comparison with the one-body one. The paper is organized as follows. In sect. 2 various treatments of the Δ-current are discussed. In sect. 3 the choice of kinematics for the present investigation is discussed. Numerical results for the cross-sections of the exclusive $^{16}\mathrm{O}(e,e'pp)^{14}\mathrm{C}$ and $^{16}\mathrm{O}(\gamma,pp)^{14}\mathrm{C}$ reactions are presented in sect. 4. Some conclusions are drawn in sect. 5.

2 The Δ-current

As has already been mentioned, the effective Δ-current operator $\boldsymbol{\jmath}_{\Delta N}$, depicted in the bottom line of fig. 1, consists of two parts, namely an excitation (I) and a de-excitation (II) part,

$$\boldsymbol{\jmath}_{\Delta N} = \boldsymbol{\jmath}^{(I)}_{\Delta N}(1,2) + \boldsymbol{\jmath}^{(II)}_{\Delta N}(1,2) + (1 \to 2) \ , \qquad (1)$$

which are given by

$$\boldsymbol{\jmath}^{(I)}_{\Delta N}(1,2) = V_{N\Delta}(1,2) G_{\Delta}(\sqrt{s_I}) \boldsymbol{\mathcal{J}}_{\Delta N}(1) \ , \qquad (2)$$

$$\boldsymbol{\jmath}^{(II)}_{\Delta N} = \boldsymbol{\mathcal{J}}_{N\Delta}(1) G_{\Delta}(\sqrt{s_{II}}) V_{\Delta N}(1,2) \ . \qquad (3)$$

In these expressions $\boldsymbol{\mathcal{J}}_{\Delta N}$, with $\boldsymbol{\mathcal{J}}_{\Delta N}=(\boldsymbol{\mathcal{J}}_{N\Delta})^{\dagger}$, describes the electromagnetic transition $\gamma N \to \Delta$. If we restrict ourselves to the dominant magnetic dipole ($M1$) transition, $\boldsymbol{\mathcal{J}}_{\Delta N}$ is given in photonuclear reactions by the matrix element

$$\langle \Delta | \boldsymbol{\mathcal{J}}_{\Delta N} | N \rangle = \frac{G^{\Delta N}_{M1}}{2M_N} i \boldsymbol{\sigma}_{\Delta N} \times \boldsymbol{k} \; e \, (\boldsymbol{\tau}_{\Delta N})_0 \ , \qquad (4)$$

where e denotes the elementary charge, $\boldsymbol{k}$ the photon momentum and M_N the nucleon mass. The spin and isospin transition operators $\boldsymbol{\sigma}_{\Delta N}$ and $\boldsymbol{\tau}_{\Delta N}$ are fixed by their reduced matrix elements $\langle \frac{3}{2} || \sigma_{\Delta N} || \frac{1}{2} \rangle = 2$ and $\langle \frac{3}{2} || \tau_{\Delta N} || \frac{1}{2} \rangle = 2$. The value of the coupling constant $G^{\Delta N}_{M1} = 4.22$ can be extracted from the elementary total photopionproduction cross-section in the Δ-region [13]. For virtual photons a usual electromagnetic dipole form factor

$$F(Q^2) = \left[1 + \frac{Q^2}{(855 \text{ MeV})^2} \right]^{-2} \qquad (5)$$

has additionally to be taken into account.

The propagator G_{Δ} in (2) depends strongly on the invariant energy $\sqrt{s}$ of the Δ. If we omit medium modifications and treat the Δ as a free particle, we use, following [14],

$$G_{\Delta}(\sqrt{s}) = \frac{1}{M_{\Delta} - \sqrt{s} - \frac{i}{2} \Gamma_{\Delta}(\sqrt{s})} \ , \qquad (6)$$

where Γ_{Δ} is the energy-dependent decay width of the Δ taken from ref. [15] and $M_{\Delta} = 1232$ MeV its mass. In the excitation part, we use for the invariant energy $\sqrt{s_I} = \sqrt{s_{NN}} - M_N$, where $\sqrt{s_{NN}}$ is the experimentally measured invariant energy of the two outgoing protons. In the de-excitation part the choice $\sqrt{s_{II}} = M_N$ turns out to be the most appropriate one [14].

We now turn to the potential $V_{N\Delta}(1,2)$, with $V_{\Delta N}(1,2) = (V_{N\Delta}(1,2))^{\dagger}$, describing the transition $N\Delta \to NN$ via meson exchange. In this work, besides the usual static π-exchange, we consider in addition also the static ρ-exchange, *i.e.*

$$V_{N\Delta} = V^{\pi}_{N\Delta} + V^{\rho}_{N\Delta} \ , \qquad (7)$$

whose explicit expressions are well known from the literature, see, *e.g.*, [16–18]:

$$\langle NN(\boldsymbol{p}') | V^{\pi}_{N\Delta} | \Delta N(\boldsymbol{p}) \rangle = -\frac{1}{(2\pi)^3} F_{\pi NN}(q^2) F_{\pi N\Delta}(q^2) \times \frac{f_{\pi NN} f_{\pi N\Delta}}{m_{\pi}^2} \boldsymbol{\tau}_{NN}(2) \cdot \boldsymbol{\tau}_{N\Delta}(1) \frac{\boldsymbol{\sigma}_{NN}(2) \cdot \boldsymbol{q} \, \boldsymbol{\sigma}_{N\Delta}(1) \cdot \boldsymbol{q}}{q^2 + m_{\pi}^2}, \qquad (8)$$

$$\langle NN(\boldsymbol{p}') | V^{\rho}_{N\Delta} | \Delta N(\boldsymbol{p}) \rangle = -\frac{1}{(2\pi)^3} F_{\rho NN}(q^2) F_{\rho N\Delta}(q^2) \times \frac{f_{\rho NN} f_{\rho N\Delta}}{m_{\rho}^2} \boldsymbol{\tau}_{NN}(2) \cdot \boldsymbol{\tau}_{N\Delta}(1) \times \frac{(\boldsymbol{\sigma}_{NN}(2) \times \boldsymbol{q}) \cdot (\boldsymbol{\sigma}_{N\Delta}(1) \times \boldsymbol{q})}{q^2 + m_{\rho}^2} \ . \qquad (9)$$

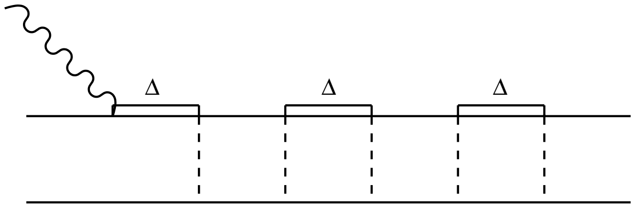

Fig. 2. A possible Δ-contribution to *pp*-knockout which is of higher order in $f_{xN\Delta}$ and leads to divergences within an unregularized approach for $V_{N\Delta}$.

In these expressions $\boldsymbol{q} = \boldsymbol{p} - \boldsymbol{p}'$, where $\boldsymbol{p}$ ($\boldsymbol{p}'$) denotes the relative momentum of the ΔN (NN) system in the initial (final) state. The quantities F_{xNN} and $F_{xN\Delta}$, $x \in \{\pi, \rho\}$, are the so-called hadronic form factors necessary for regularizing the potentials at short distances, where the meson-exchange picture becomes meaningless. As usual, they are parametrized as follows:

$$
\begin{aligned}
F_{xNN}(q^2) &= \left(\frac{\Lambda^2_{xNN} - m^2_x}{\Lambda^2_{xNN} + q^2} \right)^{n_{xNN}} , \\
F_{xN\Delta}(q^2) &= \left(\frac{\Lambda^2_{xN\Delta} - m^2_x}{\Lambda^2_{xN\Delta} + q^2} \right)^{n_{xN\Delta}} , \qquad (10)
\end{aligned}
$$

where the integers n_{xNN}, $n_{xN\Delta}$, as well as the cutoffs Λ_{xNN} and $\Lambda_{xN\Delta}$, can be treated as free parameters. In the following, various approaches are considered where different values are given to these parameters, as well as to the coupling constants f_{xNN} and $f_{xN\Delta}$.

In the simplest approach, called Δ(NoReg), we use only an unregularized pionic transition potential, *i.e.*

$$
\begin{aligned}
&\frac{f^2_{\pi NN}}{4\pi} = 0.08\, , \frac{f^2_{\pi N\Delta}}{4\pi} = 0.35\, , \Lambda_{\pi NN} = \Lambda_{\pi N\Delta} \to \infty, \\
&V^\rho_{N\Delta} = 0 \; . \qquad (11)
\end{aligned}
$$

Here, $f_{\pi N\Delta}$ has been extracted from the Δ-decay width. An unregularized pionic transition potential is used in [11, 12, 19]. This approach is similar to our previous treatment of the Δ-current, where only a simple regularization was included in coordinate space.

An unregularized transition potential can be used only if the Δ-contribution to *pp*-knockout is performed perturbatively up to the first order in $f_{\pi N\Delta}$. In a more sophisticated approach going beyond (2), additional contributions like the one depicted in fig. 2 could in principle occur, where the Δ can be excited and de-excited several times in the nuclear medium. Such mechanisms lead to serious divergences, well known from NN-scattering [16, 20], which can only be removed within a regularized treatment. The essential question is, however, how to fix, within such a refined approach, the free parameters, especially the cutoffs, in (10). In this work, we select for this purpose two alternative scenarios: NN-scattering and πN-scattering.

In a first approach, that we call $\Delta(NN)$, the parameters are fixed considering the NN-scattering in the Δ-region. For this purpose, we use a nonperturbative treatment of $V_{N\Delta}$ as outlined in some detail in [21, 22]. It turns out that a fairly good description of the NN-scattering data in the Δ-region can be achieved by choosing parameters similar to the ones of the full Bonn potential [20], *i.e.*

$$
\begin{aligned}
&\frac{f^2_{\pi NN}}{4\pi} = 0.078, && \frac{f^2_{\pi N\Delta}}{4\pi} = 0.224, \\
&\frac{f^2_{\rho NN}}{4\pi} = 7.10, && \frac{f^2_{\rho N\Delta}}{4\pi} = 20.45, \\
&\Lambda_{\pi NN} = 1300\,\text{MeV}, && \Lambda_{\pi N\Delta} = 1200\,\text{MeV}, \\
&\Lambda_{\rho NN} = 1400\,\text{MeV}, && \Lambda_{\rho N\Delta} = 1000\,\text{MeV}, \\
&n_{\pi NN} = n_{\pi N\Delta} = n_{\rho NN} = n_{\rho N\Delta} = 1 \; . && \qquad (12)
\end{aligned}
$$

In an alternative approach, the parameters of the Δ are fixed from πN-scattering in the P_{33}-channel. We call this approach $\Delta(\pi N)$. If we consider only the dominant P_{33}-channel, a suitable choice of parameters is [23]

$$
\frac{f^2_{\pi N\Delta}}{4\pi} = 1.393, \quad \Lambda_{\pi N\Delta} = 287.9\,\text{MeV}, \quad n_{\pi N\Delta} = 1 \; . \qquad (13)
$$

The values for $f_{\pi NN}$ and $\Lambda_{\pi NN}$ cannot be simply extracted from πN-scattering in the P_{33}-channel. Therefore, here we use the ones of the full Bonn potential [20], *i.e.* the same as in (12):

$$
\frac{f^2_{\pi NN}}{4\pi} = 0.078, \quad \Lambda_{\pi NN} = 1300\,\text{MeV}, \quad n_{\pi NN} = 1 \; . \qquad (14)
$$

We note that also in this approach, like in Δ(NoReg), the ρ-exchange part $V^\rho_{N\Delta}$ is switched off. We point out the dramatic differences in the values of $f_{\pi N\Delta}$ and $\Lambda_{\pi N\Delta}$ for the two treatments in (12) and (13). A more detailed discussion of this point can be found in [24–26].

In all the approaches considered till now, the Δ is treated as a free particle. In *pp*-knockout on complex nuclei, however, medium modifications in the Δ-excitation or de-excitation mechanism may occur. In order to obtain an indication of the relevance of medium effects, we follow the procedure suggested in [27] by a comparison between the $^{12}\text{C}(e, e')$ cross-section in the Δ-region and the results of the Δ-hole model [28, 29], and add a shift $V_\Delta = (-30 - 40i)$ MeV in the denominator of G_Δ (see eq. (6)), which now reads

$$
G_\Delta(\sqrt{s}) = \frac{1}{M_\Delta - \sqrt{s} - \frac{i}{2}\Gamma_\Delta(\sqrt{s}) + V_\Delta} \; . \qquad (15)
$$

In this last approach, that we call $\Delta(\pi N, \text{mod})$, we use such a modified G_Δ propagator and the same coupling constants and cutoffs as in $\Delta(\pi N)$. The shift V_Δ obtained in [27] for ^{12}C is applied here to ^{16}O, as the medium effect should not give a large difference for these two nuclei. Even if the determination of V_Δ in [27] refers to a different process and a different kinematics with respect to those chosen in this paper, we believe that an indication of the relevance of medium effects on the Δ is useful. We note that the same V_Δ was used in calculations of two-nucleon knockout reactions also in [9] and in the analysis of [30].

3 The choice of kinematics

A consistent treatment of the Δ in electromagnetic breakup reactions on complex nuclei is presently not available. The parametrizations of the effective Δ-current proposed in the previous section are therefore not "fundamental" from a certain point of view. By choosing extreme scenarios, like an unregularized *versus* strongly regularized treatments, we are able to obtain an estimate of the theoretical uncertainties. Some explicit results are presented in the next section. It is however clear from the beginning that these different parametrizations may give large numerical differences in the observables. From this point of view, one might be interested in specific kinematics where the Δ-contribution as well as its sensitivity to the different parametrizations is either maximized i) or minimized ii). Case i) allows us to pin down the most suitable Δ-parametrization in two-nucleon knockout, whereas case ii) represents in principle the cleanest scenario to extract correlation effects.

Specific kinematics where either the contribution of the one-body or of the two-body Δ-current is dominant, were already envisaged in previous studies of electromagnetic two-nucleon knockout. These kinematics can represent a good basis for the present investigation. Since, however, our main aim here is to evaluate the relevance of the unavoidable uncertainties in the Δ-contribution, it can be useful to maximize or minimize these uncertainties with the help of interference effects between the Δ and the one-body current. We may try to study this problem analytically using some simplifying assumptions. Therefore, let us ignore for the moment FSI, so that the final state of the two outgoing nucleons can be described by an antisymmetrized ($\mathcal{A}$) plane wave (PW):

$$|\psi_f\rangle_{\mathcal{A}} = |\boldsymbol{p}_1, \boldsymbol{p}_2; s_f, m_{s_f}; t_f, m_{t_f}\rangle - (-1)^{s_f+t_f} |\boldsymbol{p}_2, \boldsymbol{p}_1; s_f, m_{s_f}; t_f, m_{t_f}\rangle \ . \quad (16)$$

It is known from previous investigations that such a simple PW approximation leaves in most kinematics the qualitative features of the cross-sections unchanged. In (16), $\boldsymbol{p}_i$ denotes the asymptotic free momentum of nucleon i, while s_f and m_{s_f} label the total spin of the two outgoing nucleons and its projection, respectively. For the isospin quantum numbers t_f and m_{t_f}, in *pp*-knockout we have always $t_f = 1$ and $m_{t_f} = 1$.

In the $(e, e'pp)$ reaction the one-body current consists of three parts, namely the longitudinal charge-term (ρ) and the transverse convection ($\boldsymbol{\jmath}^{con}$) and spin ($\boldsymbol{\jmath}^{spin}$) currents. Denoting by $|\psi_i\rangle$ the relative part of the initial state with spin (isospin) quantum numbers s_i, m_{s_i} (t_i, m_{t_i}) and wave function ψ_i, the relevant matrix elements of the three terms of the one-body current are given by

$${}_{\mathcal{A}}\langle\psi_f|\rho(1)|\psi_i\rangle \sim \delta_{s_f s_i}\delta_{m_{s_f} m_{s_i}} \times \left[\psi_i\left(\boldsymbol{p} - \frac{\boldsymbol{k}}{2}\right) + (-1)^{s_f}\psi_i\left(-\boldsymbol{p} - \frac{\boldsymbol{k}}{2}\right)\right], \quad (17)$$

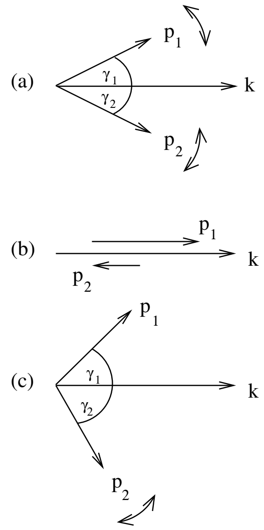

Fig. 3. Graphical illustration of the selected kinematics: (a) symmetrical kinematics with $|\boldsymbol{p}_1| = |\boldsymbol{p}_2|$, $|\gamma_1| = |\gamma_2|$; (b) super-parallel kinematics; (c) kinematics with $\gamma_1 = 45°$ fixed and γ_2 varying on the other side of the photon momentum $\boldsymbol{k}$.

$${}_{\mathcal{A}}\langle\psi_f|\boldsymbol{\jmath}^{con}(1)|\psi_i\rangle \sim \delta_{s_f s_i}\delta_{m_{s_f} m_{s_i}} \times \left[\left(\frac{2\boldsymbol{p}_1 - \boldsymbol{k}}{2M_N}\right)\psi_i\left(\boldsymbol{p} - \frac{\boldsymbol{k}}{2}\right) + (-1)^{s_f}\left(\frac{2\boldsymbol{p}_2 - \boldsymbol{k}}{2M_N}\right)\psi_i\left(-\boldsymbol{p} - \frac{\boldsymbol{k}}{2}\right)\right], \quad (18)$$

$${}_{\mathcal{A}}\langle\psi_f|\boldsymbol{\jmath}^{spin}(1)|\psi_i\rangle \sim \langle s_f m_{s_f}|i\frac{\boldsymbol{\sigma}_{NN}(1) \times \boldsymbol{k}}{2M_N}|s_i m_{s_i}\rangle \times \left[\psi_i\left(\boldsymbol{p} - \frac{\boldsymbol{k}}{2}\right) + (-1)^{s_f}\psi_i\left(-\boldsymbol{p} - \frac{\boldsymbol{k}}{2}\right)\right], \quad (19)$$

where isospin factors have been omitted for the sake of simplicity. The quantity $\boldsymbol{p}$ denotes the relative momentum of the two nucleons in the final state, *i.e.* $\boldsymbol{p} = \frac{\boldsymbol{p}_1 - \boldsymbol{p}_2}{2}$.

It is obvious from the above equations that the spin-term (19) is the ideal interference partner for the Δ-current, because both have their main contribution in the magnetic dipole ($M1$) transition. When the two protons are in a ${}^1S_0$ initial relative state, $s_i = 0$ and s_f must be necessarily 1 for the spin-current contribution (19). As a consequence, if $|\boldsymbol{p} - \frac{\boldsymbol{k}}{2}| = |-\boldsymbol{p} - \frac{\boldsymbol{k}}{2}|$, the spin-current vanishes and cannot produce any interference with the Δ-current. This is just the condition of the so-called symmetrical kinematics, depicted in the top panel of fig. 3, where the two nucleons are ejected at equal energies and equal but opposite angles with respect to the momentum transfer. As a sidemark, we would like to mention that in this kinematics, besides the spin-current, also the convection part (18) vanishes within a PW approach for a ${}^1S_0$ initial relative state.

In contrast, in the so-called super-parallel kinematics, depicted in the middle panel of fig. 3, where the two nucleons are ejected parallel and antiparallel to the momentum transfer $\boldsymbol{k}$, the difference of the arguments $|\boldsymbol{p} - \frac{\boldsymbol{k}}{2}|$ and

$|-\boldsymbol{p}-\frac{\boldsymbol{k}}{2}|$ of ψ_i in (19) is maximized for a given $\boldsymbol{k}$, and the contribution of the spin-current should become important. Therefore, we can expect that in the super-parallel kinematics also the interference between the spin- and the Δ-contribution is maximized and the existing uncertainties in the Δ-parametrization become most crucial.

These arguments, which have been brought within a PW approach and for a ${}^1S_0$ initial proton pair, should not be changed significantly by FSI and should be valid in all the situations where the ${}^1S_0$ relative partial wave gives the main contribution, such as in the ${}^{16}\mathrm{O}(e,e'pp)$ reaction to the 0^+ ground state of ${}^{14}\mathrm{C}$ [6]. Therefore, in the present investigation, cross-section calculations for the reaction ${}^{16}\mathrm{O}(e,e'pp){}^{14}\mathrm{C}_{\mathrm{g.s.}}$ have been performed in coplanar symmetrical and super-parallel kinematics, *i.e.* in two situations where the contribution of the ${}^1S_0$ relative wave, and therefore also of SRC, is emphasized [6], and where the interference effects between the one-body and the Δ-current should be minimized (symmetrical kinematics) and maximized (super-parallel kinematics).

The super-parallel kinematics chosen for the calculations is the same already considered in our previous works [2,3,6,31] and realized in the ${}^{16}\mathrm{O}(e,e'pp){}^{14}\mathrm{C}$ experiment at MAMI [32]. The incident electron energy is $E_0 = 855$ MeV, the energy transfer $\omega = 215$ MeV, and $k = 316$ MeV/c. Different values of the recoil momentum $\boldsymbol{p}_{\mathrm{B}} = \boldsymbol{k}-\boldsymbol{p}_1-\boldsymbol{p}_2$ are obtained changing the kinetic energies of the two outgoing protons. The symmetrical kinematics is calculated with the same values of E_0, ω, and k, the kinetic energies of the two outoing nucleons are determined by energy conservation and different values of p_{B} are obtained changing the scattering angles of the two protons.

Two different kinematics are considered also for the reaction ${}^{16}\mathrm{O}(\gamma,pp){}^{14}\mathrm{C}_{\mathrm{g.s.}}$: a coplanar symmetrical kinematics with an incident photon energy $E_\gamma = 400$ MeV, and the coplanar kinematics depicted in the bottom panel of fig. 3 with $E_\gamma = 120$ MeV, where the energy and the scattering angle of the first outgoing proton are fixed, at $T_1 = 45$ MeV and $\gamma_1 = 45°$, respectively; the kinetic energy of the second proton is determined by energy conservation, and different values of p_{B} are obtained by varying the scattering angle γ_2 of the second outgoing nucleon on the other side of the photon momentum. This choice of kinematics for the (γ,pp) reaction is determined by the results of our previous works [3,7]. It was found in [7] that the symmetrical kinematics is dominated by the Δ-current, whereas the contribution of the one-body spin- and convection-currents is only of minor importance. Therefore, this case is interesting to give direct access to the Δ-contribution in a situation where interference effects between the one-body and the Δ-current are expected to be small. Note the difference in the symmetrical kinematics for (γ,pp) and $(e,e'pp)$: as discussed above, in both cases the contributions of the transverse convection- and spin-current are suppressed, but in $(e,e'pp)$ also the longitudinal charge-term contributes and is dominant, as will become apparent in the next section. On the other hand, in the kinematics at $E_\gamma = 120$ MeV both one-body and Δ-current contributions are important [3]. Therefore, this case can be helpful to investigate the interplay between one-body and two-body currents in the (γ,pp) reaction.

The effect of the mutual interaction between the two outgoing nucleons (NN-FSI) has been studied in [2,3] within a perturbative approach. The contribution of NN-FSI depends on the kinematics and on the type of electromagnetic probe, and in particular situations produces a significant enhancement of the calculated cross-section [2,3]. Work is in progress to include this contribution within a more accurate treatment. Detailed studies not outlined here have shown now that NN-FSI do not disturb qualitatively the conclusions concerning the Δ-current drawn below. Consequently, NN-FSI can be safely neglected in this work.

4 Results

The cross-section of the exclusive ${}^{16}\mathrm{O}(e,e'pp){}^{14}\mathrm{C}$ and ${}^{16}\mathrm{O}(\gamma,pp){}^{14}\mathrm{C}$ reactions have been calculated in the kinematics discussed in the previous section. The theoretical model is the same already presented in [5,6,31].

The basic ingredients of the calculation are the matrix elements of the nuclear charge-current operator between initial and final nuclear many-body states, *i.e.*,

$$J^\mu(\boldsymbol{k}) = \int \langle \Psi_f | j^\mu(\boldsymbol{r}) | \Psi_i \rangle e^{i\boldsymbol{k}\cdot\boldsymbol{r}} \mathrm{d}\boldsymbol{r} \ . \qquad (20)$$

Bilinear products of these integrals give the components of the hadron tensor, whose suitable combinations give all the observables available from the reaction process [1].

The model is based on the two assumptions of an exclusive knockout reaction: the direct mechanism and the transition to a specific discrete state of the residual nucleus [5,6,33]. Thus, we consider a direct one-step process where the electromagnetic probe directly interacts with the pair of nucleons that are emitted and the $A-2 \equiv B$ nucleons of the residual nucleus behave as spectators. Recent experiments [32,34–40] on reactions induced by real and virtual photons have confirmed the validity of this mechanism for low values of the excitation energy of the residual nucleus.

As a result of these two assumptions, the integrals (20) can be reduced to a form with three main ingredients: the two-nucleon overlap function (TOF) $|\psi_i\rangle$ between the ground state of the target and the final state of the residual nucleus, the nuclear current j^μ of the two emitted nucleons, and the two-nucleon–scattering wave function $|\psi_f\rangle$.

The treatment of the nuclear current operator has been discussed in sect. 2. In the final-state wave function $|\psi_f\rangle$ only the interaction of each of the two nucleons with the residual nucleus is included. Therefore, the scattering state is written as the product of two uncoupled single-particle distorted wave functions, eigenfunctions of a complex phenomenological spin and energy-dependent optical potential [41].

The TOF $|\psi_i\rangle$ contains information on nuclear structure and correlations and in principle requires a calculation of the two-hole spectral function including consistently SRC as well as long-range correlations (LRC), mainly due to collective excitations of nucleons at the nuclear surface. It is well known from previous work that the cross-sections are generally sensitive to the treatment of correlations. Different approaches are used in [5,6,31,42]. Since the main aim of the present work is to study the uncertainties in the treatment of the Δ-current in combination with the effect of correlations, it can be interesting to compare results obtained with different TOFs. Therefore, the present calculations have been performed with the three different approaches used in refs. [5,6,31].

In the simpler approach of [5] the TOF is given by the product of a coupled and antisymmetrized shell model pair function and a Jastrow-type central and state-independent correlation function taken from [43]. In this approach (SM-SRC) only SRC are considered and the final state of the residual nucleus is a pure two-hole state. For instance, the ground state of ^{14}C is a $(p_{1/2})^{-2}$ hole in ^{16}O.

In the more sophisticated approaches of [6] and [31] the TOFs are obtained from the two-proton spectral function of ^{16}O with a two-step procedure which includes both SRC and LRC. In the first step, LRC are calculated in a shell model space large enough to account for the main collective features of the pair removal amplitude. The single-particle propagators used for this dressed random phase approximation (RPA) description of the two-particle propagator include the effect of both LRC and SRC. In the second step, that part of the pair removal amplitudes which describes the relative motion of the pair is supplemented by defect functions, which contain SRC, obtained by solving the Bethe-Goldstone equation with a Pauli operator which considers only configurations outside the model space where LRC are calculated. Different defect functions are obtained for different relative states using different realistic NN-potentials. In the approach of [6,44] (SF-A), the nonlocality of the Pauli operator is neglected, resulting in a set of only few defect functions, which are essentially independent of the center-of-mass (CM) motion of the pair. In the more recent approach of [31] (SF-B) the Pauli operator is computed exactly, resulting in a larger number of defect functions which have a more complicate state dependence. Moreover, in [31] the evaluation of nuclear structure effects related to the fragmentation of the single-particle strength has been improved by applying a Faddeev technique to the description of the internal propagators in the nucleon self-energy [45,46]. The defect functions used in the present calculations are obtained from the Bonn-A NN-potential for the SF-A approach and from Bonn-C for SF-B. It was found, however, in [6] that defect functions from the Bonn-A and Bonn-C potentials do not produce significant differences.

The results for the ^{16}O$(e,e'pp)^{14}$C$_{\text{g.s.}}$ reaction in the symmetrical kinematics are displayed in fig. 4. The shape of the recoil-momentum distribution is driven by the CM orbital angular momentum L of the knocked-out pair. This feature, that is fulfilled in a factorized PW approach, is not spoiled by FSI [5,6]. Different partial waves of relative and CM motion are included in the TOF. For the considered transition to the 0^+ ground state of ^{14}C, the main components of relative motion are: $^1S_0$, combined with

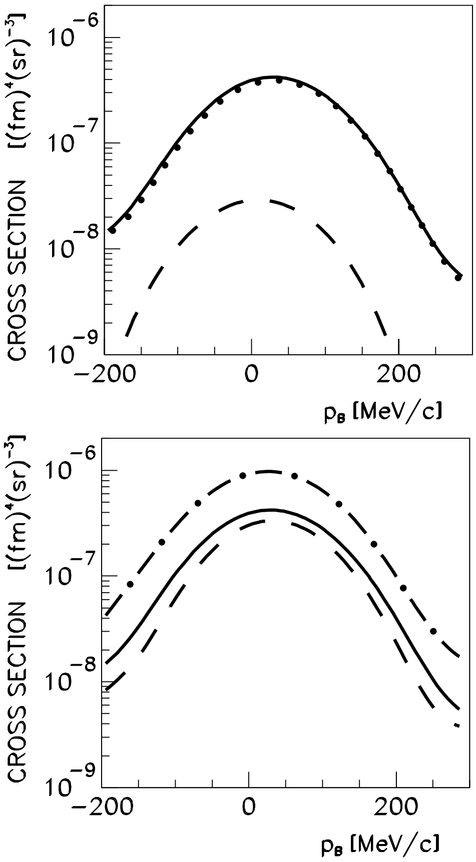

Fig. 4. The differential cross-section of the ^{16}O$(e,e'pp)$ reaction to the 0^+ ground state of ^{14}C as a function of the recoil momentum p_{B} in a coplanar symmetrical kinematics with E_0 = 855 MeV, an electron-scattering angle θ_e = 18°, ω = 215 MeV, and k = 316 MeV/c. Different values of p_{B} are obtained changing the scattering angles of the two outgoing protons. Positive (negative) values of p_{B} refer to situations where $\boldsymbol{p}_{\text{B}}$ is parallel (antiparallel) to $\boldsymbol{k}$. The $\Delta(NN)$ parametrization is used in the calculations. In the top panel the TOF is taken from the SF-B approach and separate contributions of the one-body and Δ-current are shown by the dotted and dashed line, respectively. The solid curve gives the final result. The results with different TOFs are shown in the bottom panel: SF-B (solid line), SF-A (dashed line), and SM-SRC (dash-dotted line).

$L = 0$, and $^3P_1$, combined with $L = 1$. The shape of the cross-sections in fig. 4 clearly indicates the dominance of the $^1S_0$, $L = 0$, component. The separate contributions of the one-body and Δ-current, displayed in the top panel of the figure, show that the Δ-contribution is very small. In practice, the whole cross-section is due to the one-body current, in particular to its longitudinal charge-term. The contribution of the convection- and spin-terms is practically negligible. The results in the top panel are obtained with the TOF from the SF-B approach and with the $\Delta(NN)$ parametrization. Different TOFs and Δ-parametrizations do not change the qualitative features of the calculated cross-sections. Different parametrizations affect only the contribution of the Δ-current (dashed line),

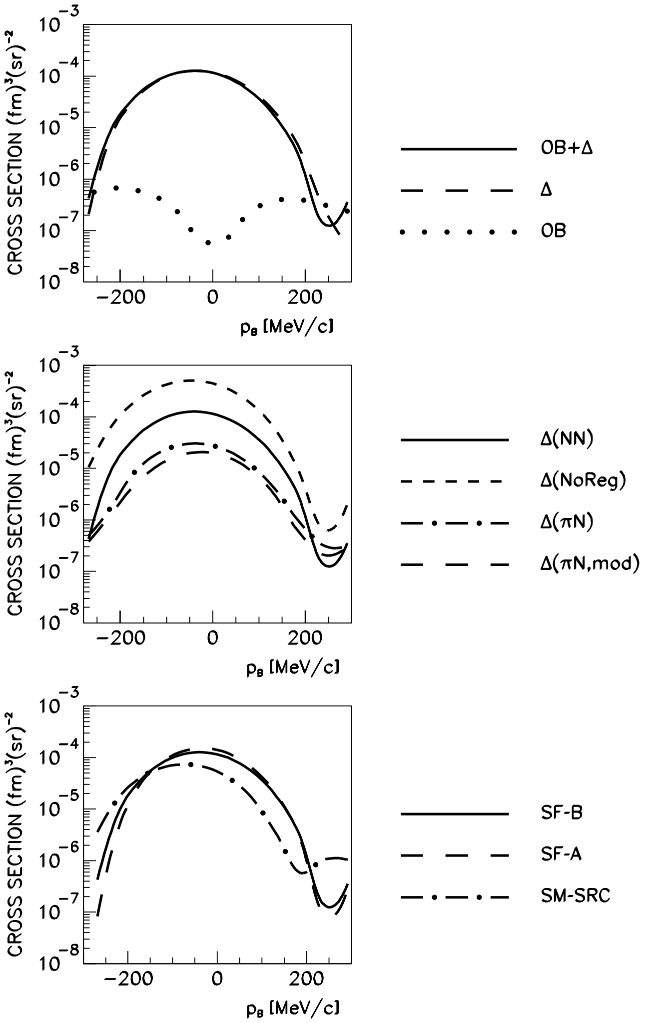

Fig. 5. The differential cross-section of the ^{16}O$(\gamma, pp)^{14}$C$_{\text{g.s.}}$ reaction as a function of the recoil momentum p_{B} in a coplanar symmetrical kinematics with $E_\gamma = 400$ MeV. In the top panel the separate contributions of one-body (OB) and Δ-currents are displayed and compared with the total cross-section. In the middle panel the results with different Δ-parametrizations are compared. In both panels the TOF is taken from the SF-B approach. In the bottom panel the results with different TOFs are compared.

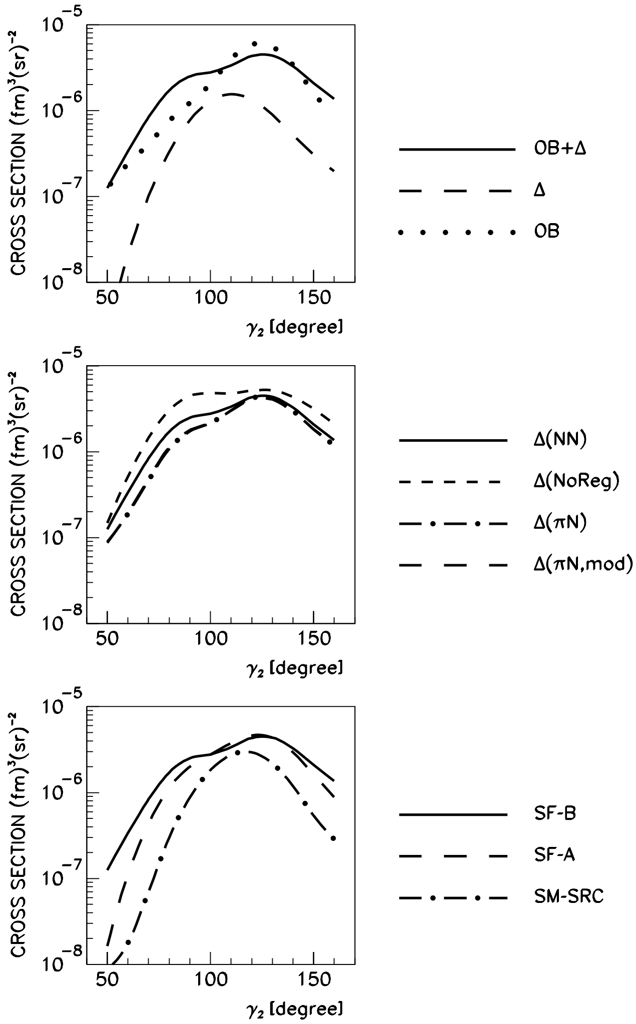

Fig. 6. The differential cross-section of the ^{16}O$(\gamma, pp)^{14}$C$_{\text{g.s.}}$ reaction as a function of the scattering angle γ_2 of the second outgoing proton in a coplanar kinematics with $E_\gamma = 120$ MeV, $T_1 = 45$ MeV, and $\gamma_1 = 45°$. The results are presented in the same way as in fig. 5.

but do not affect the final result, that is dominated by the longitudinal part of the one-body current (dotted line). Thus, in this case the results are insensitive to the uncertainties in the treatment of the Δ. Quantitative differences are produced by the three TOFs. The results displayed in the bottom panel show that different treatments of correlations do not change the shape but only the size of the cross-section. The SM-SRC result (dash-dotted line) is $\sim$ 2–3 times larger than SF-B (solid line), that, in turn, is between 20% and 40% larger than SF-A (dashed line).

The cross-section of the ^{16}O$(\gamma, pp)^{14}$C$_{\text{g.s.}}$ reaction in the symmetrical kinematics at $E_\gamma = 400$ MeV, displayed in fig. 5, is completely dominated by the Δ-contribution (dashed line in the top panel). This qualitative result is obtained with all the Δ-parametrizations and TOFs considered in the present work. The shape of the recoil-momentum distribution confirms also in this case the dominance of the $^1S_0$, $L = 0$, partial wave. It is interesting to notice, however, that the separate contribution of the one-body current (dotted line in the top panel) is driven by the $L = 1$ component. This result can be understood if we consider that in a reaction induced by a real photon only the transverse components of the current contribute. It has been demonstrated in sect. 3 that in a symmetrical kinematics the transverse part of the one-body current is strongly suppressed when the two protons are in an initial $^1S_0$ relative state. Thus, the $^3P_1$, $L = 1$, component gives the main contribution to the one-body current. This contribution is, however, overwhelmed in the final cross-section by the Δ-current. Differences larger than one order of magnitude in the peak region are produced by the different Δ-parametrizations (middle panel). The largest cross-section is given by the Δ(NoReg) prescription, but large differences are also found between the $\Delta(NN)$ and $\Delta(\pi N)$ results. The modified propagator in $\Delta(\pi N, \text{mod})$ gives only a slight reduction of the cross-section calculated with the $\Delta(\pi N)$ parametrization. The results produced by the TOFs from the SF-A and SF-B spectral functions are very close (bottom panel). A slight reduction and a somewhat different shape is obtained with the simpler SM-SRC approach. The difference in the shape is due to the larger contribution of the $^3P_1$, $L = 1$, component in SM-SRC. The differences of the results with the three TOFs in the two symmetrical kinematics in figs. 4 and 5 are due to the different effects of correlations on the one-body current in the $(e, e'pp)$ cross-section, and on the two-body Δ-current in the (γ, pp) reaction.

The results for the $^{16}\text{O}(\gamma, pp)^{14}\text{C}_{\text{g.s.}}$ reaction in the kinematics at $E_\gamma = 120$ MeV are displayed in fig. 6. In this kinematics, where both convection- and spin-terms are important, the one-body current (top panel, dotted line) gives the main contribution to the cross-section. The effect of the Δ-current (dashed line), however, is not negligible: it produces a significant enhancement of the $^3P_1$ component and a slight reduction of the $^1S_0$ one. Such a reduction is due to the destructive interference between the spin- and the Δ-current contributions in the $^1S_0$ relative state. The final result is that the Δ affects both the size and the shape of the cross-section. The shape is determined by the combined effect of the $L = 0$ and $L = 1$ CM components. The uncertainties due to the various Δ-parametrizations (middle panel) are within a factor of ~ 2. The cross-sections calculated with the $\Delta(\pi N)$ parametrization and with the modified propagator in $\Delta(\pi N, \text{mod})$ overlap in the figure. The SF-A and SF-B results (bottom panel) are generally very close. The differences at lower angles are produced by the $^3P_1$ component. A substantial reduction of the calculated cross-section is obtained with the simpler SM-SRC approach.

The cross-sections for the $^{16}\text{O}(e, e'pp)^{14}\text{C}_{\text{g.s.}}$ reaction in the super-parallel kinematics are displayed in fig. 7. The results obtained with different TOFs and Δ-parametrizations are compared in the figure. Dramatic differences are found between the unregularized and the regularized treatments of the Δ-current. The Δ-contribution is given in the right panels of fig. 7. When it is calculated with the $\Delta(\text{NoReg})$ approach (short-dashed line) it differs both in size and shape from the results of the three regularized versions, that are in general close to each other. The final cross-section, given by the sum of the one-body and the Δ-current, calculated in the $\Delta(\text{NoReg})$ approach turns out to be generally larger than the cross-section due only to the one-body current (dotted line). In contrast, the regularized Δ-parametrizations give, in combination with the one-body current, strong destructive interference effects and the final cross-section is generally lower than the contribution of the one-body current. The relevance of such a destructive interference depends on the relative weight of the one-body and Δ-current contributions, that is different with the different TOFs. For each TOF similar results are obtained with the three regularized Δ-currents. The differences between the results of unregularized and regularized treatments in the final cross-section depend on the TOF and can be large.

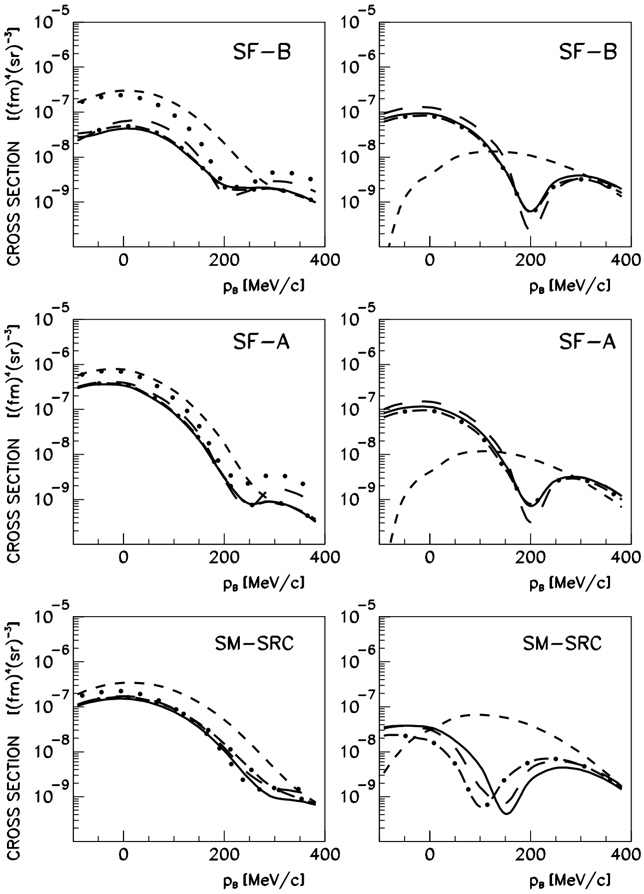

Fig. 7. The differential cross-section of the $^{16}\text{O}(e, e'pp)^{14}\text{C}_{\text{g.s.}}$ reaction as a function of the recoil momentum p_B in a super-parallel kinematics with $E_0 = 855$ MeV, $\theta_e = 18°$, $\omega = 215$ MeV, and $k = 316$ MeV/c. Different values of p_B are obtained changing the kinetic energies of the outgoing nucleons. Positive (negative) values of p_B refer to situations where $\boldsymbol{p}_\text{B}$ is parallel (antiparallel) to $\boldsymbol{k}$. The results with different TOFs (SF-B, SF-A, and SM-SRC) are given. In the right panels the separate contributions of the two-body Δ-current are shown. The final results given by the sum of the one-body and Δ-currents are shown in the left panels, where the dotted lines give the separate contribution of the one-body current. The different Δ-parametrizations are displayed by solid ($\Delta(NN)$), short-dashed ($\Delta(\text{NoReg})$), dash-dotted ($\Delta(\pi N)$), and long-dashed ($\Delta(\pi N, \text{mod})$) lines.

The SF-A and SF-B approaches produce different one-body contributions. A substantial reduction for low values of the recoil momentum is obtained with SF-B [31]. In contrast, the Δ-contributions obtained in the two models are very similar. Thus, with SF-B the separate contributions of the one-body and Δ-current are of about the same size, while with SF-A the one-body contribution is larger than the one due to the Δ. As a consequence, a stronger destructive interference, as well as a larger difference between the results of the regularized and unregularized prescriptions, is found with SF-B. The uncertainties

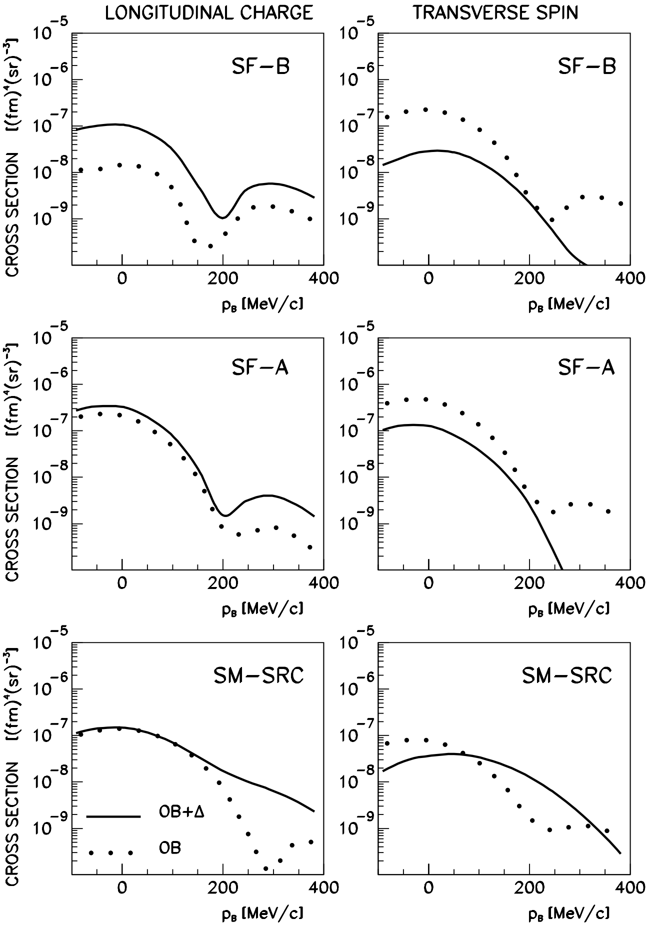

Fig. 8. The differential cross-section of the $^{16}\mathrm{O}(e,e'pp)^{14}\mathrm{C}_{\mathrm{g.s.}}$ reaction in the super-parallel kinematics with different TOFs (SF-A, SF-B, and SM-SRC). The dotted lines show the contribution of the one-body longitudinal charge- (left panels) and transverse spin-current (right panels). The solid lines give the results where the two-body Δ-current, calculated with the $\Delta(NN)$ parametrization, is added to the corresponding one-body contribution.

due to the Δ-treatment are strongly reduced with SF-A and become even smaller with the simpler SM-SRC approach. We point out the large differences obtained with the three TOFs both in the size and shape of the calculated cross-sections. These differences are due to the different treatments of correlations in the three models, and are emphasized in this particular super-parallel kinematics by the interference between the one-body and the Δ-current.

Some arguments concerning interference effects between the Δ and the one-body current have been already discussed in sect. 3. The numerical results obtained in the symmetrical and super-parallel kinematics of the $(e,e'pp)$ reaction confirm those arguments. In order to illustrate the conclusions of sect. 3 with a specific numerical example and to understand more thoroughly the results of fig. 7, we compare in the left and right panels of fig. 8 the separate contributions of the one-body longitudinal charge- and transverse spin-currents obtained with the three TOFs (dotted lines). The sum of each term with the Δ-current is also shown in the figure (solid lines). The contribution of the one-body convection-current is negligible and is not considered here. The calculations presented in the figure are performed with the $\Delta(NN)$ prescription. Similar results are obtained with $\Delta(\pi N)$ and $\Delta(\pi N,\mathrm{mod})$.

It has been demostrated in sect. 3 that the contribution of the one-body spin-term, that is minimized in symmetrical kinematics, becomes important in super-parallel kinematics. This result is confirmed by the results of fig. 8. The comparison between the one-body charge and spin-current contributions shows that the spin-current contribution is generally larger than the one-body longitudinal charge-current one. With the SF-B approach the spin-current contribution turns out to be larger by one order of magnitude. It is interesting to notice that the one-body longitudinal-current contribution calculated in the SF-B approach is about one order of magnitude lower than with SF-A, while only a factor ~ 2 is found between the SF-A and SF-B results for the one-body spin-current. This explains the different results given by the two TOFs for the full one-body currents in fig. 7 and in [31]. When added to the one-body longitudinal term, the Δ-current produces an enhancement of the cross-section that is large with SF-B, where the one-body contribution of the longitudinal term is small, and small with SF-A, where the one-body longitudinal contribution is much larger. A different effect is given by the Δ in combination with the spin-term. Here it produces a strong destructive interference that is larger with SF-B than with SF-A. Similar results are found with all the regularized Δ-parametrizations. In contrast, no destructive interference effect is obtained with the Δ(NoReg) prescription. This explains the results of fig. 7.

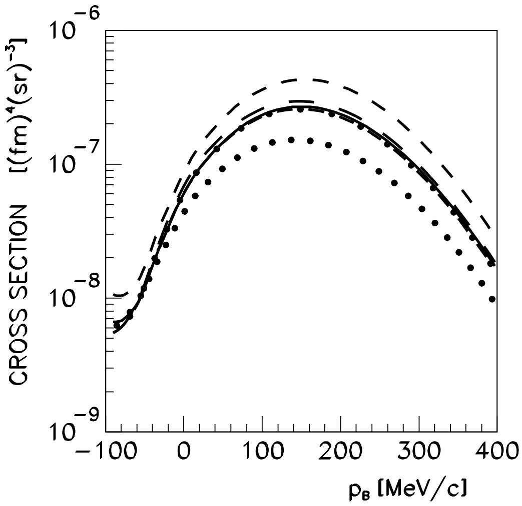

Fig. 9. The differential cross-section of the $^{16}\mathrm{O}(e,e'pp)$ reaction to the 1^+ excited state at 11.31 MeV of $^{14}\mathrm{C}$ in the same super-parallel kinematics as in fig. 7. The TOF is taken from the SF-B approach. The dotted line gives the separate contribution of the one-body current, the other lines the final result with different Δ-parametrizations: $\Delta(NN)$ (solid line), Δ(NoReg) (short-dashed line), $\Delta(\pi N)$ (dash-dotted line), $\Delta(\pi N,\mathrm{mod})$ (long-dashed line).

The results displayed in fig. 8 with the SF-A and SF-B approaches are dominated by the $^1S_0$ component, that is responsible for the destructive interference between the one-body spin- and Δ-current contributions. For the $^3P_1$ component the Δ gives always an enhancement of the one-body cross-section. The somewhat different results shown in fig. 8 with the SM-SRC two-nucleon wave function are due to the heavier weight of the $^3P_1$ component in this approach.

The effects of the different Δ-parametrizations in the ^3P states can be seen in fig. 9, where the cross-section of the ^{16}O$(e,e'pp)$ reaction to the 1^+ excited state of ^{14}C is displayed in the same super-parallel kinematics as in fig. 7. For this transition only ^3P states contribute: $^3P_0,^3P_1,^3P_2$, all combined with $L=1$. The Δ-current produces a substantial enhancement of the cross-section calculated with the one-body current. The two separate contributions are of about the same size and add up in the cross-section. Only slight differences are given by the regularized Δ-parametrizations. A larger cross-section is given by the Δ(NoReg) prescription. The differences, however, are within a factor of about 2.

5 Summary and conclusions

The combined effect of the two-body Δ-current and correlations has been discussed in electro- and photo-induced exclusive two-proton knockout reactions from ^{16}O.

The Δ-current operator consists of an excitation and a de-excitation part. The potential describing the transition $N\Delta \to NN$ via meson exchange contains the π- and ρ-exchange. Results with unregularized and regularized transition potentials have been compared in order to evaluate the theoretical uncertainties in the Δ-contribution. Different parametrizations of the effective Δ-current have been proposed. The parameters for the regularized prescriptions are fixed alternatively from πN- and NN-scattering in the Δ-region. Nuclear medium effects have been included through a shift in the Δ-propagator suggested by a comparison between inclusive electron-scattering data in the Δ-region and the results of the Δ-hole model.

Correlations are included in the two-nucleon overlap function within different approaches. In a simpler treatment the overlap function is given by the product of a shell model pair wave function and of a Jastrow-type correlation function. In a more sophisticated model the overlap function is obtained from the calculation of the two-proton spectral function. The results of two different calculations are compared, where the spectral function has been evaluated in the framework of a many-body approach with a realistic nuclear force, and where short-range and long-range correlations are taken into account consistently with a two-step procedure.

In the final state only the interaction of each of the two nucleons with the residual nucleus is included through an optical potential fitted to elastic proton-nucleus scattering. The mutual interaction between the outgoing nucleons (NN-FSI) is neglected, because it is irrelevant for the qualitative understanding of the Δ-current in the different considered kinematics.

Many different kinematics can in principle be considered. With a few numerical examples we have shown that in different situations different reaction mechanisms can be relevant and the various ingredients of the calculations can affect the cross-section in a different way. Thus, a suitable choice of kinematics can allow us to reduce the uncertainties on the theoretical ingredients and disentangle the specific contributions.

There are situations, like the symmetrical kinematics in electron scattering, where the contribution of the one-body current through correlations is dominant, while the Δ-contribution is very small and therefore the cross-section is insensitive to the uncertainites in the treatment of the Δ-current. Such situations appear very well suited to probe correlations, even though the size and shape of the cross-section mainly depend in this case on the momentum distribution of the proton pair inside the nucleus.

There are also situations, like the symmetrical kinematics in photoreactions at intermediate energy, where the contribution of the one-body current is suppressed and the cross-section is dominated by the Δ-current. In this case the cross-section is very sensitive to the treatment of the Δ and to its parameters. Such situations appear well suited to study the Δ-current in the nucleus and can be helpful to pin down the most suitable parametrization.

We have shown that there are also kinematics in photoreactions at lower energy where the contribution of the one-body current is competitive and even larger than the contribution of the Δ-current. In this case both contributions are important, but the interference between them is small and the uncertainties due to different Δ-parametrizations are not large. Such situations can be helpful to investigate correlations in alternative to or, preferably, in combination with electron scattering.

Finally, we have considered the case of the super-parallel kinematics in the $(e,e'pp)$ reaction. Here the cross-section gets a large contribution from both one-body and two-body currents and their interference can be crucial in the final result. The peculiarity of the super-parallel kinematics is that an important role is played in the one-body current by the transverse spin-term, whose contribution is generally larger than the one due to the longitudinal charge-term. The spin-current has a magnetic dipole form which can strongly interfere with the dominant term of the Δ-current when the two protons are in an initial $^1S_0$ relative state. These interference effects can be crucial in the final cross-section when the $^1S_0$ component dominates the reaction process, like in the case of the transition to the ground state of ^{14}C. This behavior of the super-parallel kinematics is completely different from the symmetrical kinematics, where the spin-current is negligible and the cross-section is dominated by the charge-term.

We have found that in the super-parallel kinematics the interference between the spin- and the Δ-current in the $^1S_0$ state is always destructive when a regularized prescription is used for the Δ and that different regularized

Δ-parametrizations give similar results. In contrast, an unregularized current has a different behavior and gives no destructive interference with the spin-current. The difference depends mainly on the relative weight of the longitudinal and spin-terms, that, in turn, depends on the treatment of correlations in the overlap function.

Different overlaps can produce large differences in the contribution of the longitudinal charge-current, which is essentially an antisymmetrized amplitude given by the Fourier transform of the correlation function. When the charge contribution becomes small, the negative interference due to the spin-current makes the cross-section small and a reduction of up to one order of magnitude can be obtained with respect to the one-body contribution. When the charge contribution is large, it is able to counterbalance the negative interference and the final cross-section becomes larger.

We have found that suitable kinematics can be envisaged to study the different ingredients entering the cross-section and the different reaction mechanisms of electromagnetic two-proton knockout reactions.

Situations where the longitudinal part of the one-body current is dominant and the uncertainties in the treatment of the Δ-current are negligible are well suited to study short-range correlations. Peculiar interesting effects and a strong sensitivity to correlations are found in kinematics where the different terms of the nuclear current compete and interfere. If we want, however, to extract unambiguous information on correlations, it is indispensable that all the theoretical ingredients of the reaction are under control and, in particular to resolve the uncertainties in the Δ-contribution. To this purpose, situations where the Δ-contribution is dominant can also be envisaged, that are useful to study the behavior of the Δ-current in the nucleus.

In conclusion, electromagnetic two-proton knockout reactions contain a wealth of information on correlations and on the behavior of the Δ-current in a nucleus, but it seems to be impossible to extract this interesting information just from one or two "ideal" kinematics. Consequently, experimental data are needed in various kinematics which mutually supplement each other. Concerning the different kinematics studied in this work, we are of course aware that a suitable one for a theoretical analysis is not necessarily the best one for an experimental measurement. Since comparison between theory and data is necessary, close and continuous collaboration between theorists and experimentalists is therefore essential to achieve a satisfactory understanding of electromagnetic two-proton knockout and to determine all the ingredients contributing to the cross-section.

This work has been supported by the Deutsche Forschungsgemeinschaft (SFB 443), by the Istituto Nazionale di Fisica Nucleare (INFN) and by the Italian MIUR through the PRIN *Fisica Teorica del Nucleo Atomico e dei Sistemi a Molti Corpi*. M. Schwamb would like to thank the Dipartimento di Fisica Nucleare e Teorica of the University of Pavia for the warm hospitality during his stays in Pavia.

References

1. S. Boffi, C. Giusti, F.D. Pacati, M. Radici, *Electromagnetic response of atomic nuclei*, in *Oxford Studies in Nuclear Physics* (Clarendon Press, Oxford, 1996).
2. M. Schwamb, S. Boffi, C. Giusti, F.D. Pacati, Eur. Phys. J. A **17**, 7 (2003).
3. M. Schwamb, S. Boffi, C. Giusti, F.D. Pacati, Eur. Phys. J. A **20**, 233 (2004).
4. S. Boffi, C. Giusti, F.D. Pacati, Phys. Rep. **266**, 1 (1993).
5. C. Giusti, F.D. Pacati, Nucl. Phys. A **615**, 373 (1997).
6. C. Giusti, F.D. Pacati, K. Allaart, W.J.W. Geurts, W.H. Dickhoff, H.M. Müther, Phys. Rev. C **57**, 1691 (1998).
7. C. Giusti, F.D. Pacati, Nucl. Phys. A **641**, 297 (1998).
8. M. Vanderhaeghen, L. Machenil, J. Ryckebusch, M. Waroquier, Phys. Lett. B **316**, 17 (1993).
9. J. Ryckebusch, V. Van der Sluys, K. Heyde, H. Holvoet, W. Van Nespen, M. Waroquier, M. Vanderhaeghen, Nucl. Phys. A **624**, 581 (1997).
10. J. Ryckebusch, W. Van Nespen, Eur. Phys. J. A **20**, 435 (2004).
11. M. Anguiano, G. Co', A.M. Lallena, J. Phys. G **29**, 1119 (2003).
12. M. Anguiano, G. Co', A.M. Lallena, Nucl. Phys. A **744**, 168 (2004).
13. R. Schmidt, diploma thesis, Mainz, 1995.
14. P. Wilhelm, H. Arenhövel, C. Giusti, F.D. Pacati, Z. Phys. A **359**, 467 (1997).
15. B.H. Brandsen, R.G. Moorhouse, *The Pion-Nucleus System* (Princeton University Press, Princeton, NJ, 1973).
16. R. Machleidt, Adv. Nucl. Phys. **19**, 189 (1989).
17. H. Garcilazo, T. Mizutani, *πNN Systems* (World Scientific, Singapore, 1990).
18. M. Vanderhaeghen, L. Machenil, J. Ryckebusch, M. Waroquier, Nucl. Phys. A **580**, 551 (1994).
19. J.E. Amaro, G. Co', A.M. Lallena, Ann. Phys. (N.Y.) **221**, 306 (1993).
20. R. Machleidt, K. Holinde, Ch. Elster, Phys. Rep. **149**, 1 (1987).
21. P. Wilhelm, Dissertation, Mainz, 1992.
22. M. Schwamb, H. Arenhövel, Nucl. Phys. A **690**, 647 (2001).
23. H. Pöpping, P.U. Sauer, X.-Z. Zang, Nucl. Phys. A **474**, 557 (1987).
24. H. Tanabe, K. Ohta, Phys. Rev. C **31**, 1876 (1985).
25. Ch. Elster, K. Holinde, D. Schütte, R. Machleidt, Phys. Rev. C **38**, 1828 (1988).
26. G. Holzwarth, R. Machleidt, Phys. Rev. C **55**, 1088 (1997).
27. C.R. Chen, T.-S.H. Lee, Phys. Rev. C **38**, 2187 (1988).
28. J.H. Koch, E.J. Moniz, N. Ohtsuka, Ann. Phys. (N.Y.) **154**, 99 (1984).
29. J.H. Koch, N. Ohtsuka, Nucl. Phys. A **435**, 765 (1985).
30. I.J.D. MacGregor *et al.*, Phys. Rev. Lett. **80**, 245 (1998).
31. C. Barbieri, C. Giusti, F.D. Pacati, W.H. Dickhoff, Phys. Rev. C **70**, 014606 (2004).
32. G. Rosner, Prog. Part. Nucl. Phys. **44**, 99 (2000).
33. C. Giusti, F.D. Pacati, Nucl. Phys. A **535**, 573 (1991).
34. C.J.G. Onderwater *et al.*, Phys. Rev. Lett. **78**, 4893 (1997).
35. C.J.G. Onderwater *et al.*, Phys. Rev. Lett. **81**, 2213 (1998).
36. R. Starink *et al.*, Phys. Lett. B **474**, 33 (2000).
37. J.C. McGeorge *et al.*, Phys. Rev. C **51**, 1967 (1995).
38. Th. Lamparter *et al.*, Z. Phys. A **355**, 1 (1996).
39. J.D. McGregor *et al.*, Phys. Rev. Lett. **80**, 245 (1998).

40. D.P. Watts *et al.*, Phys. Rev. C **62**, 014616 (2000).
41. A. Nadasen *et al.*, Phys. Rev. C **23**, 1023 (1981).
42. D.N. Kadrev, M.V. Ivanov, A.N. Antonov, C. Giusti. F.D. Pacati, Phys. Rev. C **68**, 014617 (2003).
43. C.C. Gearhart, PhD Thesis, Washington University, St. Louis (1994); C.C. Gearhart, W.H. Dickhoff, private communication.
44. W.J.W. Geurts, K. Allaart, W.H. Dickhoff, H. Müther, Phys. Rev. C **53**, 2207 (1996).
45. C. Barbieri, W.H. Dickhoff, Phys. Rev. C **63**, 034313 (2001).
46. C. Barbieri, W.H. Dickhoff, Phys. Rev. C **65**, 064313 (2002).